Macromolecular Research, Vol. 14, No. 5, pp 491-498 (2006)

Thermal Degradation Kinetics of Antimicrobial Agent, Poly(hexamethylene guanidine) Phosphate

Sangmook Lee* and Byung Suk Jin

Department of Applied Chemistry, Dongduk Women's University, Seoul 136-714, Korea

Jae Wook Lee

Applied Rheology Center, Department of Chemical Engineering, Sogang University, Seoul 121-742, Korea

Received March 13, 2006; Revised August 11, 2006

Abstract: The thermal degradation of poly(hexamethylene guanidine) phosphate (PHMG) was studied by dynamic thermogravimetric analysis (TGA) and pyrolysis-GC/MS (p-GC). Thermal degradation of PHMG occurs in three different processes, such as dephosphorylation, sublimation/vaporization of amine compounds and decomposition/recombination of hydrocarbon residues. The kinetic parameters of each stage were calculated from the Kissinger, Friedman and Flynn-Wall-Ozawa methods. The Chang method was also used for comparison study. To investigate the degradation mechanisms of the three different stages, the Coats-Redfern and the Phadnis-Deshpande methods were employed. The probable degradation mechanism for the first stage was a nucleation and growth mechanism, A_n type. However, a power law and a diffusion mechanism, D_n type, were operated for the second degradation stage, whereas a nucleation and growth mechanism, A_n type, were operated again for the third degradation stage of PHMG. The theoretical weight loss against temperature curves, calculated by the estimated kinetic parameters, well fit the experimental data, thereby confirming the validity of the analysis method used in this work. The life-time predicted from the kinetic equation is a valuable guide for the thermal processing of PHMG.

Keywords: poly(hexamethylene guanidine) phosphate, thermal degradation kinetics, thermogravimetric analysis, pyrolysis-GC/MS, life-time.

Introduction

The group of promising antiseptic cationic surfactants includes poly(hexamethylene guanidine) (PHMG) salts. The biocidal properties of PHMG are related to the presence of guanidine groups in the repeating unit of this polymer shown in Scheme I.

Scheme I

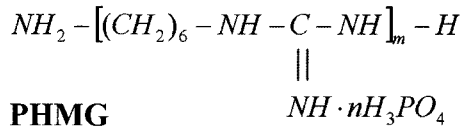

PHMG

PHMG exhibiting strong bactericidal activity can be used in textile for suppressing growing microorganisms,[1] in medicine for disinfection of medical fiber or film materials,[2-5] in operating and injection fields, in agriculture in storage of vegetables, in lumber industry as fungicides and preservatives, in wastewater treatment, in protection of metals from corrosion, biological overgrowing, and salt deposition,[6] etc.

In spite of excellent antimicrobial properties of PHMG, its thermal properties are very poor, which make high temperature processing difficult. Thermal degradation kinetics and mechanisms of PHMG must be fully understood for successful processing in high temperature and various applications. For thermal degradation kinetics, thermogravimetric analysis (TGA) has been used widely.[7-10] Kinetic data obtained from TGA are very useful for understanding the thermal degradation processes and mechanisms. Surprisingly, there were only a few publications on PHMG though it has attracted considerable attention as highly efficient biocidal and nontoxic agents.

In this study, the thermal degradation of PHMG was investigated by dynamic TGA and pyrolysis-GC/MS (p-GC) to understand the degradation phenomena during the polymer processing with PHMG. Firstly, four methods were used to carry out the thermal degradation kinetics of PHMG. Secondly, thermal degradation mechanism was determined by solid-state decomposition reaction mechanisms. Thirdly,

*Corresponding Author. E-mail: smlee@dongduk.ac.kr

the theoretically calculated weight loss curves from the estimated kinetic parameters are compared to the experimental values. Finally, the life-time prediction at certain temperature were suggested.

Theoretical Approach

Generally, the thermal degradation reaction of a solid material can be shown as: B(solid)→C(solid)+D(gas) where B(solid) is the starting material, D(solid) and C(gas) are the different products during the disappearance of B(solid). In thermogravimetric measurements, the isothermal degradation rate $d\alpha/dt$ is assumed as a linear function of the rate constant, $k(T)$, and a function of the conversion, $f(\alpha)$:

$$\frac{d\alpha}{dt} = k(T)f(\alpha) \tag{1}$$

k is the reaction constant, which can be expressed by the Arrhenius equation:

$$k(T) = k_0 e^{-E/RT} \tag{2}$$

where k_0 is the pre-exponential factor, E_a is the activation energy, R is the gas constant, and T is absolute temperature. α is the degree of conversion, which can be defined as follows:

$$\alpha = \frac{w_0 - w_t}{w_0 - w_f} \tag{3}$$

where w_0 is the initial weight of dry sample, w_t are the actual mass of the sample at instant t and w_f is the final weight of the sample at the end of the TGA. Combining eqs. (1) and (2) we have

$$\frac{d\alpha}{dt} = k_0 e^{-E/RT} f(\alpha) \tag{4}$$

For dynamic thermal degradation at constant heating rate $\beta = dT/dt$, eq. (4) transforms to

$$\frac{d\alpha}{dt} = \frac{dT}{dt}\frac{d\alpha}{dT} = \beta\frac{d\alpha}{dT} = k_0 e^{-E/RT} f(\alpha) \tag{5}$$

Activation energy E_a can be calculated by various methods.

Differential Methods. *Kissinger method* determines the activation energy simply without a precise knowledge of the reaction mechanism involved:

$$\ln\frac{\beta}{T_p^2} = \ln\frac{k_0 R}{E_a} + \ln[n(1-\alpha_p)^{n-1}] - \frac{E_a}{RT_p} \tag{6}$$

where β is the heating rate, T_p and α_p the temperature and the conversion at maximum weight -loss rate, respectively. By the plot of $\ln(\beta/T_p^2)$ against $1/T_p$, the activation energy can be determined from the slope.[10] *Friedman method* is probably the most general of the differential techniques and utilizes the following natural logarithmic equation:

$$\ln\left(\beta\frac{d\alpha}{dt}\right) = \ln[k_0 f(\alpha)] - \frac{E_a}{RT} \tag{7}$$

By plotting $\ln[\beta(d\alpha/dT)]$ against $1/T$ for a constant α value, the value of the $-E_a/R$ can be obtained directly.[11] *Chang method* employed the following equation:

$$\ln\frac{\beta(d\alpha/dT)}{(1-\alpha)^n} = \ln k_0 - \frac{E_a}{RT} \tag{8}$$

A plot of $\ln[\beta(d\alpha/dT)/(1-\alpha)^n]$ against $1/T$ can yield a straight line only if the reaction order n is correctly selected. The slope is $-E_a/R$ and the intercept is $\ln k_0$.[12]

Integral Methods. *Flynn-Wall-Ozawa method* is one of the "model-free" integral methods that can determine the activation energy without knowledge of reaction order:

$$\log\beta = \log\frac{k_0 E_a}{g(\alpha)R} - 2.315 - \frac{0.457E_a}{RT} \tag{9}$$

The activation energy can be calculated from a $\log\beta$ versus $1/T$ for given values of conversion.[13] *Coats-Redfern method* used an approximation for the resolution of eq. (5), obtaining

$$\ln\frac{g(\alpha)}{T^2} = \ln\frac{k_0 R}{\beta E_a} - \frac{E_a}{RT} \tag{10}$$

According to the different degradation processes, with the theoretical function $g(\alpha)$,[14] Plot of $\ln[g(\alpha)/T^2]$ versus $1/T$ gives the slope for evaluation of the activation energy E_a, as well as the reaction mechanism.[14] *Phadnis-Deshpande method* can determine the dependence of reaction mechanism on the functional form of α:

$$g'(\alpha) = \int\frac{1}{f(\alpha)g(\alpha)}d\alpha = -\frac{E_a}{RT} \tag{11}$$

With the functions of $g'(\alpha)$,[14] the activation energy E_a can be calculated from the plot of $g'(\alpha)$ against $1/T$, and the reaction mechanism can be evaluated.[14]

Experimental

Materials. PHMG (SKYBIO 1100, M_w=3,000, *PDI*=3.0, T_g=101 °C, phosphoric acid content=6 wt%) in the form of powder was supplied by SK Chemicals Co., Ltd., Korea. It was dried in vacuum oven prior to characterization. The chemical structure of PHMG is shown in Scheme I.

Thermogravimetric Analysis. Thermogravimetric analysis (TGA) was performed employing TGA (TA Q-series, U.S.A.). Samples of about 10 mg were heated from 50 to 550 °C at various heating rates (2, 5, 10, 20, 30, and 50 °C/

min) in flowing nitrogen gas of 40 mL/min in a thermobalance.

Pyrolysis-GC/MS (p-GC). The pyrolysis-GC/MS (p-GC) analysis was examined to investigate the thermal degradation phenomena. The pyrolysis was carried out by a pyrolyzer (model 2020iD, Frontier laboratories). The exit gas was analyzed on-line by a gas chromatograph (model 6890 GC, Agilent) equipped with ultra alloy-5 capillary column with stationary phase (5% diphenyl and 95% dimethyl polysiloxane) and a mass spectrometer (5973N MSD, HP). The samples were pyrolyzed at 230, 350, and 400 °C in Helium. The initial time and the interface temperature were 30 sec and 350 °C, respectively. The effluent from pyrolyzer was split with the ratio of 100:1 and the flow rate of 89.5 mL/min. The temperature of GC was increased from 50 to 320 °C at a rate of 10 °C/min.

Results and Discussion

Thermal Degradation. Thermal degradation of PHMG was studied by determining its weight loss during heating. The weight loss (%) under a steady flow of nitrogen gas at six different heating rates, and their derivatives were shown in Figure 1(a) and Figure 1(b), respectively. In the thermogravimetic (TG) curves and the derivatives of thermogravimetric (DTG) curves three different degradation processes were observed. Therefore, the degradation kinetics was carried out to investigate the degradation mechanisms for three degradation stages.

Table I summarized the results of TGA for PHMG. As the heating rate increased, degradation onset temperatures defined as the onset temperatures of the DTG curves and three peak temperatures increased. This temperature shift might be due to heat transfer effect.[15] On the other hand, the residual char yield decreased as the heating rate increased. It could be explained by the process of rapid or flash pyrolysis[16] which need very high heating rate and short residence time of reactants and products. They yield very little residual solid but large quantities of tar.

Pyrolysis-GC/MS (p-GC). To investigate the three degradation stages pyrolysis-GC/MS was carried out for PHMG at three different temperatures of 230, 350, and 400 °C.

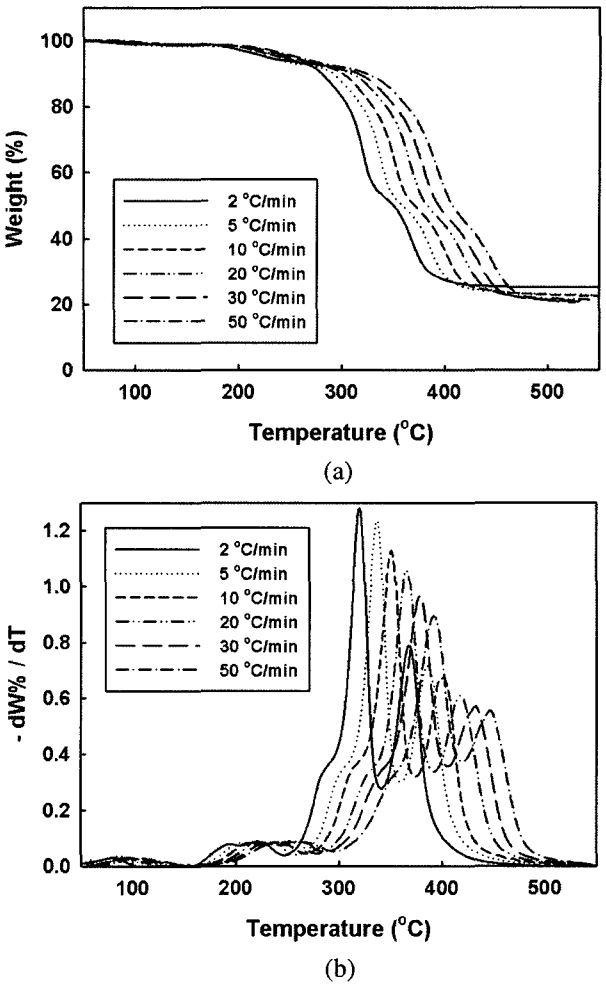

Figure 1. Dynamic thermogravimetric curves (a) and their derivatives (b) at different heating rates.

From the pyrogram at 230 °C any meaningful information could not be obtained due to low temperature. Instead of p-GC, however, from TGA graph, there was seen about 6.2 wt% of mass loss in the first degradation stage and this amount agreed with the content of phosphoric acid, 6 wt%, in PHMG. Thus the mass loss in the first degradation stage might be due to dephosphorylate. Two pyrograms for

Table I. Dynamic Thermogravimetric Data of PHMG

Heating Rate (°C/min)	Degradation Onset Temperature (°C)	Maximum Degradation Temperature (°C)			Residue (wt%)
		1st	2nd	3rd	
2	155	222	320	368	25.13
5	159	234	337	386	22.77
10	175	241	351	401	22.40
20	184	253	366	418	21.33
30	191	259	379	433	20.78
50	194	266	392	448	20.59

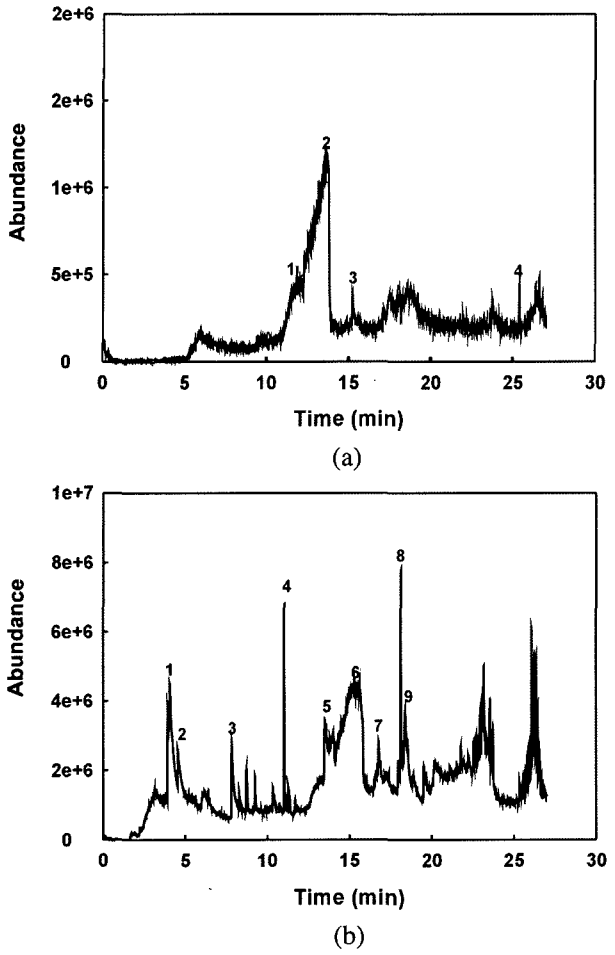

Figure 2. The pyrograms of gas chromatography for PHMG at 350 °C (a) and 400 °C (b).

PHMG at 350 and 400 °C were shown in Figure 2(a) and Figure 2(b), respectively and the characteristic peaks were assigned and listed in Table II. The major pyrolates at 350 °C were hexamethylene imine (about 61%), while those at 400 °C were various hydrocarbons. Thus the second degradation stage might be attributed to sublimation/vaporization of amine compounds and the third degradation stage might be due to decomposition/recombination of the mixture of hydrocarbon residues.

Degradation Kinetics. Kissinger, Friedman, and Flynn-Wall-Ozawa method were employed to calculate the activation energies from TGA data of PHMG because they were independent of any degradation mechanism (i.e., "model-free") and were used most widely. Using Kissinger method, the values of activation energy for three peaks were obtained from the slope of $\ln(\beta/T_p^2)$ against $1{,}000/T_p$ plot with correlation coefficient greater than 0.9966, shown in Figure 3. The values of activation energy also could be determined from Friedman kinetic plots of $\ln(\beta(d\alpha/dT))$ against $1{,}000/T$, shown in Figure 4. A set of straight lines was obtained at different conversion, with the slope of each line being $-E_a/R$ with correlation coefficient greater than 0.9740. By Flynn-Wall-Ozawa method, eq. (9), the log β versus $-1{,}000/T$ plots from 4 to 90% conversion for the degradation of PHMG were shown in Figure 5. The lines at different conversion values in each stage, the lines were approximately parallel to each other and all the correlation coefficients of linearity in calculation of each activation energy were larger than 0.9783.

The activation energies obtained from above three methods were summarized in Table III. The activation energy values obtained from Kissinger method were somewhat lower than the values from other two methods especially in the first stage.

Table II. Characteristic Peaks for the Pyrogram of PHMG

T (°C)	Peak No.	Time (min)	Area %	Components
350	1	12.55	21.84	hexamethylene imine
	2	13.29	39.33	hexamethylene imine
	3	15.21	10.38	[S-(E)]-2,6-dimethyl-4-octene
	4	25.38	5.69	3,7,11-trimethyl-2,6,10-dodecatriene-1-ol
400	1	4.06	14.78	2-methyl-1,3-pentadiene
	2	4.55	4.18	2-ethyl-1,3-butadiene
	3	7.83	5.34	1,6-hexanediamine
	4	11.02	4.52	2-octene
	5	14.49	0.28	hexamethylene imine
	6	15.17	1.35	hexamethylene imine
	7	16.78	1.16	cis-4-decene
	8	18.12	7.97	(E)-2-nonene
	9	18.38	6.36	2,6-dimethyl-cyclohexanone

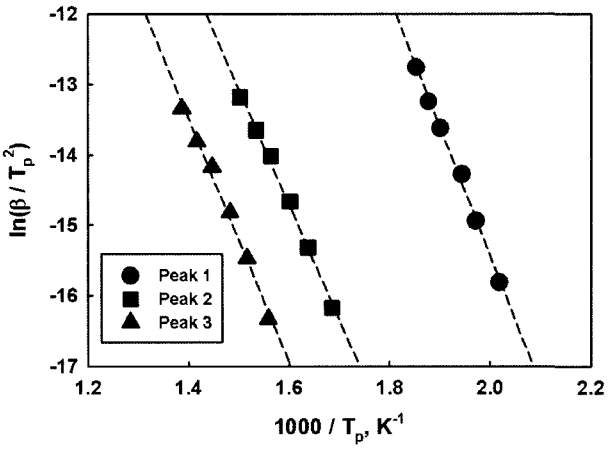

Figure 3. Kissinger plots at varying conversion.

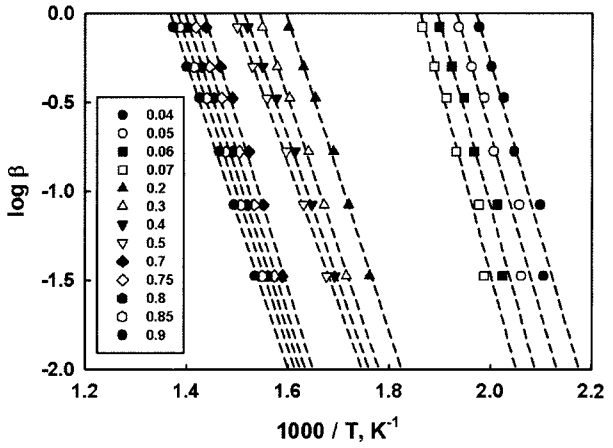

Figure 5. Flynn-Wall-Ozawa plots at varying conversion.

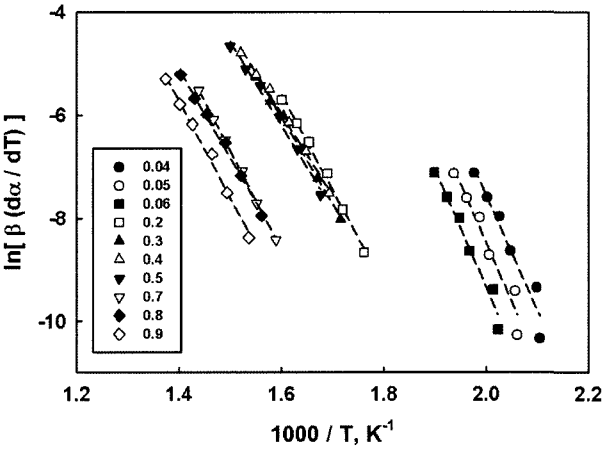

Figure 4. Friedman plots at varying conversion.

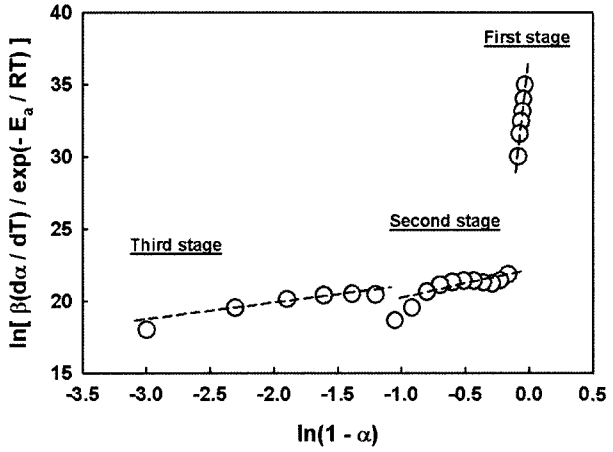

Figure 6. Friedman calculation for determination of reaction order and pre-exponential factor at heating rate 2 °C/min.

For the first stage, even though the correlation coefficient of Kissinger plot was greater than 0.9966, the first peak on the DTG curve was not sharp enough to determine the peak point clearly and this broadness might bring some difference. The values of activation energies decreased in the following order: the first stage > the third stage > the second stage.

The pre-exponential factor, k_0 and the degradation reaction order, n could be obtained from the plot based on Friedman method, eq. (7). The values of activation energies were averaged for each stage as 175, 142, and 151 kJ/mol, respectively. The plot based on Friedman method $\ln[\beta(d\alpha/dT)/\exp(-E_a/RT)]$ against $\ln(1-\alpha)$[17] were shown in Figure 6. From the slope and the intercept, the degradation reaction order, n and the pre-exponential factors, k_0 could be calculated for each stage. The summary of the kinetic parameters at a heating rate of 2 °C/min was shown in Table IV.

For comparative study, the activation energy by Chang method was calculated from the plot of $\ln[\beta(d\alpha/dT)/(1-\alpha)^n]$ against $1{,}000/T$ and was shown in Figure 7. The reaction order, n was chosen as 2.09 when the correlation coefficient was maximum value, 0.9791. The activation energy and the

Table III. Activation Energies of PHMG for Various Methods

Method	1st Stage		2nd Stage		3rd Stage	
	E_a (kJ/mol)	r	E_a (kJ/mol)	r	E_a (kJ/mol)	r
Kissinger	152	0.9983	136	0.9979	143	0.9966
Friedman	188	0.9740	139	0.9960	150	0.9962
Flynn-Wall-Ozawa	185	0.9783	151	0.9984	161	0.9980

pre-exponential factor calculated from the slope and the intercept were also presented in Table IV. These parameters were used to compare experimental data with numerical simulation.

Kinetic Mechanism. The activation energies obtained from above three "model-free" methods (Kissinger, Friedman, and Flynn-Wall-Ozawa) could be used to validate the thermal degradation mechanism. The Coats-Redfern and Phadnis-Deshpande methods were employed to investigate the thermal degradation mechanism of PHMG by comparing the activation energies obtained from the three methods. For different function $g(\alpha)$ based on Coats-Redfern method, the activation energies were calculated at a heating rate of 2 °C/min from the plot of $\ln[g(\alpha)/T^2]$ against $1{,}000/T$, listed in Table V. Similarly, those for different $F(\alpha)$ based on Phadnis-Deshpande method were obtained from the plot of $F(\alpha)$ versus $1{,}000/T$, presented in Table VI.

Comparing the activation energies in Table V with the three methods, the values from Kissinger method, 152 kJ/mol were very close to 153 kJ/mol from A_4 nucleation and growth mechanism for the first stage. For the second stage, those from Friedman and Flynn-Wall-Ozawa methods were corresponded to a D_n diffusion type. The thermal degradation mechanism

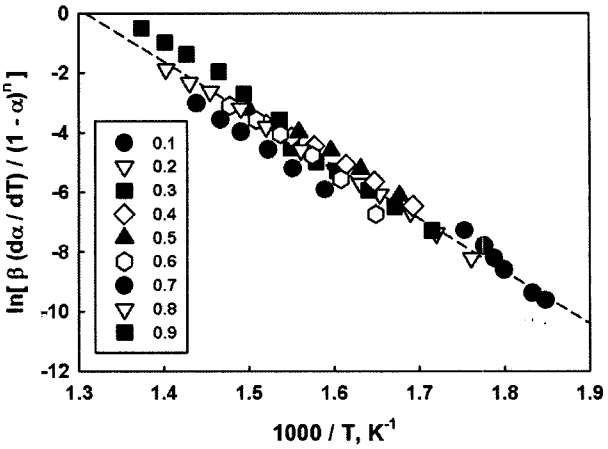

Figure 7. Chang plots at varying conversion.

for the third stage was a A_n type and the best agreement with Flynn-Wall-Ozawa method corresponded to 163 kJ/mol from a A_2 nucleation and growth mechanism with the best correlation 0.9869.

In addition to Coats-Redfern method, Padnis-Deshpande method was also employed to confirm the thermal degrada-

Table IV. Kinetic Parameters for the Degradation of PHMG Using Three-Stage Model and Chang Model at 2 °C/min

	Three-Stage Model			Chang Model
	1st Stage	2nd Stage	3rd Stage	
Activation Energy, E_a (kJ/mol)	175	142	151	146
Pre-exponential Factor, k_0 (s^{-1})	2.30×10^{16}	5.51×10^{9}	5.73×10^{9}	9.41×10^{9}
Degradation Reaction Order, n	87.94	2.84	1.39	2.09

Table V. Activation Energies of PHMG Calculated from the Coats-Redfern Method for Solid-State Process Mechanisms at 2 °C/min

Mechanism	1st Stage		2nd Stage		3rd Stage	
	E_a (kJ/mol)	r	E_a (kJ/mol)	r	E_a (kJ/mol)	r
A_2	73	0.9900	167	0.9870	163	0.9869
A_3	113	0.9908	256	0.9874	249	0.9874
A_4	153	0.9911	344	0.9876	336	0.9877
R_1	31	0.9861	66	0.9909	21	0.9739
R_2	-	-	2	0.4774	30	0.9616
R_3	-	-	-	-	21	0.9493
D_1	71	0.9893	141	0.9920	53	0.9832
D_2	71	0.9896	149	0.9906	77	0.9880
D_3	72	0.9898	158	0.9889	116	0.9893
D_4	71	0.9896	152	0.9900	89	0.9892
F_1	32	0.9871	79	0.9856	76	0.9851
F_2	-	-	19	0.8479	146	0.9604
F_3	-	-	47	0.8931	303	0.9629

Table VI. Activation Energies of PHMG Obtained from the Phadnis-Deshpande Method for Solid-State Process Mechanisms at 2 °C/min

Mechanism	1st Stage		2nd Stage		3rd Stage	
	E_a (kJ/mol)	r	E_a (kJ/mol)	r	E_a (kJ/mol)	r
Power law [Eq.(1)]	39	0.9916	75	0.9928	32	0.9884
Power law [Eq.(2)]	79	0.9916	150	0.9928	64	0.9884
Phase boundary [Eq.(3)]	40	0.9919	84	0.9899	63	0.9910
Phase boundary [Eq.(4)]	40	0.9918	81	0.9907	54	0.9914
Nucleation and Growth [Eq.(5)]	81	0.9921	177	0.9882	173	0.9884
Nucleation and Growth [Eq.(6)]	121	0.9921	265	0.9882	260	0.9884
Nucleation and Growth [Eq.(7)]	162	0.9921	353	0.9882	346	0.9884
Valensi, 2-D Diffusion [Eq.(8)]	79	0.9918	158	0.9916	87	0.9908
Jander, 3-D Diffusion [Eq.(9)]	80	0.9919	167	0.9899	127	0.9910
Brounshtein-Ginstling, 3-D Diffusion [Eq.(10)]	80	0.9918	161	0.9910	100	0.9914

tion mechanism of PHMG. Among the three methods, only the value from Kissinger method was the nearest to a nucleation and growth type for the first stage. The expected mechanisms for the second stage were power law (2) and 2-D diffusion and they were corresponded to Flynn-Wall-Ozawa method. For the third stage, Flynn-Wall-Ozawa method was agreed the best with nucleation growth mechanism.

Numerical Simulation. To confirm the validity of the fit using the three stage model and Chang model, dynamic TG curve and theoretical values calculated from the models were compared at heating rate 2 °C/min. The nth order kinetic equation with initial condition α=0 at T=155 °C was solved numerically by Runge-Kutta 4th order method using the kinetics parameters. It was observed that though the Chang model predicted fairly the experiment, three-stage model did much better the experimental data, shown in Figure 8. Furthermore, Chang model poorly predicted initial degradation region below inflection temperature. On the other hand, three-stage model showed slight deviations near the transition ranges between stages. This might be attributed to the significant change of the kinetic parameters in this region.

Thermal Stability During Processing. There were many problems in processing of PHMG due to its weak thermal stability. Therefore the estimation of the optimum processing temperature and the life-time would provide a very useful information. The thermal degradation kinetics equation, eq. (4) could be integrated and rearranged for time:

$$t = \frac{1-(1-\alpha)^{1-n}}{k(1-n)}$$

According to eq. (5), the life-time was calculated and was shown in Figure 9. The life-time of PHMG were found to decrease with the increasing temperature. For instance, the life-time of PHMG under 200 °C were calculated to be about below 30 sec to reach conversion 0.1 (equivalent to about

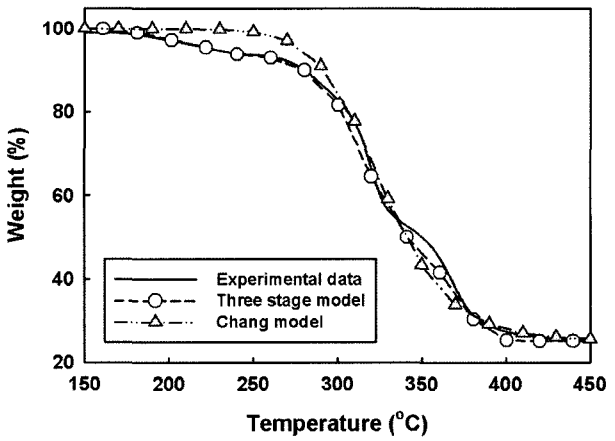

Figure 8. Comparison between simulation and experimental data at heating rate 2 °C/min.

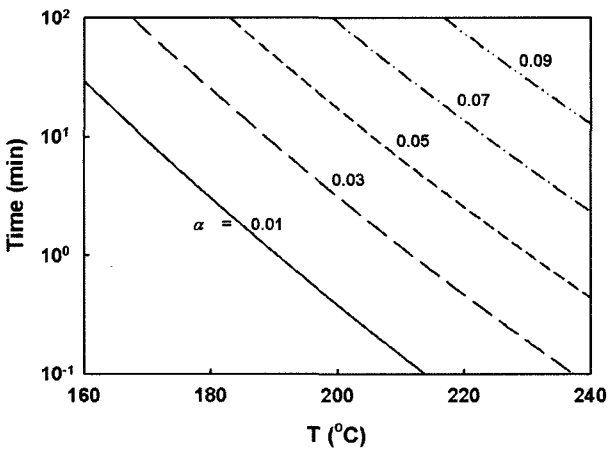

Figure 9. Life-time versus temperature at varying conversion.

0.75% weight reduction for PHMG) and this might mean that PHMG can be processed for 30 sec at 200 °C without significant degradation. Although practically, several additional degradation processes like mechanical and chemical degradation would cooperatively shorten the life-time of PHMG, the life time from thermal degradation kinetics would give a guide for processing of PHMG.

Conclusions

To investigate the degradation phenomena and the stability during thermal processing of antimicrobial agent, PHMG the thermal degradation study was carried out by dynamic TGA data and pyrolysis-GC/MS. From the analysis of pyrolysis-GC/MS three degradation stages might be due to dephosphorylate, sublimation/vaporization of amine compounds and decomposition/recombination of hydrocarbon residues, respectively.

The kinetic parameters of the three degradation stages were evaluated by using four methods. The activation energies of the first degradation stage calculated from by Kissinger, Friedman, and Flynn-Wall-Ozawa methods were 152, 188, and 185 kJ/mol, respectively. The average activation energy (E_a), pre-exponential factor (k_0), and reaction order (n) were 175 kJ/mol, 2.3×10^{16} s^{-1}, and 87.9, respectively. For the second stage, the activation energies were 136, 139, and 151 kJ/mol, respectively. The average E_a, k_0 ,and n were 142 kJ/mol, 5.5×10^9 s^{-1}, and 2.8, respectively. For the third stage, the activation energies were 143, 150, and 161 kJ/mol, respectively. The average E_a, k_0, and n were 151 kJ/mol, 5.7×10^9 s^{-1}, and 1.4, respectively.

The probable thermal degradation mechanism from Coats-Redfern and Phadnis-Deshpande methods was a nucleation and growth mechanism, A_n type, for the first degradation stage of PHMG. However, its second degradation stage followed a power law and a diffusion mechanism, D_n type. On the other hand, its third degradation stage corresponded to a nucleation and growth mechanism, A_n type, again.

By using the estimated kinetic parameters, the predicted weight loss against temperature curves well fit the experimental data, which supported the validity of estimated parameters and applicability of the analysis method used in this work. Finally, from the kinetic equation, the optimum processing times at varying temperature and conversion were calculated. This life time curves would suggest an easy way to predict the thermal stability during processing of PHMG.

Acknowledgements. The authors acknowledge Mr. Jeong-Joo Shin and Mr. Gaeng Wook Yang of SK Chemicals Co., Ltd., Korea, who supplied PHMG and the valuable information about it.

References

(1) M. A. Chapurina, L. V. Redna, T. N. Yudanova, K. P. Khomyakov, T. A. Cherdyntseva, and A. I. Netrusov, *Fibre Chem.*, **36**, 30 (2004).
(2) T. N. Yudanova, I. F. Skokova, O. N. Bochkareva, and L. S. Gal'braikh, *Fibre Chem.*, **33**, 282 (2001).
(3) E. Yu. Aleshina, T. N. Yudanova, and I. F. Skokova, *Fibre Chem.*, **33**, 421 (2001).
(4) M. S. Khil, H. Y. Kim, Y. S. Kang, H. J. Bang, and D. R. Lee, *Macromol. Res.*, **13**, 62 (2005).
(5) W. S. Shim, J. S. Lee, and D. S. Lee, *Macromol. Res.*, **13**, 344 (2005).
(6) L. M. Antonik, V. A. Lopyrev, N. A. Korchevin, and V. P. Tomin, *Russ. J. Appl. Chem.*, **75**, 257 (2002).
(7) B. Saha and A. K. Ghoshal, *Chem. Eng. J.*, **111**, 39 (2005).
(8) X. Li, M. Huang, and Y. Yang, *Polym. Int.*, **48**, 1277 (1999).
(9) Z. Gao, I. Amasaki, and M. Nakada, *J. Anal. Appl. Pyrol.*, **67**, 1 (2003).
(10) H. E. Kissinger, *Anal. Chem.*, **29**, 1702 (1957).
(11) J. P. Lin, C. Y. Chang, C. H. Wu, and S. M. Shih, *Polym. Degrad. Stabil.*, **53**, 295 (1996).
(12) W. L. Chang, *J. Appl. Polym. Sci.*, **53**, 1759 (1994).
(13) T. J. Ozawa, *Therm. Anal.*, **2**, 301 (1970).
(14) J. T. Sun, Y. D. Huang, G. F. Gong, and H. L. Cao, *Polym. Degrad. Stabil.*, **91**, 339 (2006).
(15) S. Volker and Th. Rieckmann, *J. Anal. Appl. Pyrol.*, **62**, 165 (2002).
(16) J. Lede, *Ind. Eng. Chem. Res.*, **39**, 893 (2002).
(17) H. L. Friedman, *J. Polym. Sci. C*, **6**, 183 (1964).